Journal of the Korean Ceramic Society
Vol. 53, No. 2, pp. 253~257, 2016.

http://dx.doi.org/10.4191/kcers.2016.53.2.253

Properties of Working Electrodes with Nano $YBO_3:Eu^{3+}$ Phosphor in a Dye Sensitized Solar Cell

Yunyoung Noh, Minkyoung Choi, Kwangbae Kim, and Ohsung Song†

Department of Materials Science and Engineering, University of Seoul, Seoul 02504, Korea

(Received November 23, 2015; Revised November 27, 2015; Accepted January 12, 2016)

ABSTRACT

We added 0 ~ 5 wt% $YBO_3:Eu^{3+}$ nano powders in a scattering layer of a working electrode to improve the energy conversion efficiency (ECE) of a dye sensitized solar cell (DSSC). FESEM and XRD were used to characterize the microstructure and phase. PL and micro Raman were used to determine the fluorescence and the composition of $YBO_3:Eu^{3+}$ phosphor. A solar simulator and a potentiostat were used to confirm the photovoltaic properties of the DSSC with $YBO_3:Eu^{3+}$. From the results of the microstructure and phase of the fabricated $YBO_3:Eu^{3+}$ nano powders, we identified $YBO_3:Eu^{3+}$ having particle size less than 100 nm. Based on the microstructure and micro Raman results, we confirmed the existence of $YBO_3:Eu^{3+}$ in the scattering layer and found that it was dispersed uniformly. Through photovoltaic properties results, the maximum ECE was shown to be 5.20%, which can be compared to the value of 5.00% without $YBO_3:Eu^{3+}$. As these results are derived from conversion of light in the UV range into visible light by employing $YBO_3:Eu^{3+}$ in the scattering layer, these indicate that the ECE of a DSSC can be enhanced by employing an appropriate amount of $YBO_3:Eu^{3+}$.

Key words : Dye sensitized solar cells, Scattering layer, Energy conversion efficiency, $YBO_3: Eu^{3+}$

1. Introduction

As one of the next-generation solar cells, the dye sensitized solar cell (DSSC) has the advantage of low-cost, large scale fabrication, and flexible substrate applicability.[1] However, whereas energy conversion efficiency (ECE) of the Si solar cell is about 20%,[2] that of DSSC is about relatively low at about 11%,[3] requiring further research into solving this problem.

The DSSC consists of working electrode (WE), electrolyte, and counter electrode (CE).[4-6] In case of WE, dye plays a role as forming electrons and holes upon absorbing light, and the formed electrons are delivered to an external circuit through TiO_2 layers.[7] Hence, WE engineering significantly affects the ECE of DSSCs. In particular, in order to improve the ECE, absorbing light from outside as much as possible is important.

To enhance light energy absorption, two major ways are utilized: one is to improve the quantity of absorption through WE engineering; and the other is to enhance the absorb range of ultra-violet rays and infrared rays as well as the existing visible-light range.

First, as for the way of light energy absorption through WE engineering, D. Huang *et al.* [8] have reported an increase in the ECE to 5.25% compared with the exiting 3.81% by adding diatoms into the mesoporous TiO_2 layer in order to increase specific surface area. Y. Noh *et al.* [9] reported that an existing ECE of 5.25% increased to 6.35% by using a scattering layer which reflects penetrated light and makes re-absorption possible.

Second, in order to absorb the range of ultra-violet rays and infrared rays as well as the existing visible-light range, the up-conversion and down-conversion method is available. The up-conversion method converts long waves in the infrared range into visible rays while the down-conversion method converts short waves in the ultraviolet range into visible rays. Since the down-conversion method is easier, utilizing phosphor that absorb the ultraviolet range is more effective.[10] N. Yao *et al.*[11] applied ZnO: Eu^{3+}, Dy^{3+} phosphor that absorbs short waves of 338 nm and 395 nm and then emits waves of 458 nm and 611 nm to DSSCs, which improved the ECE up to 4.48% higher than the existing 1.3%. S. Bai *et al.*[12] added perylene into an electrolyte that absorbs short waves of 350 ~ 440 nm and emits a visible-light waves as wide as 450 ~ 550 nm so that it can absorb the ultraviolet range of light further, which improved the ECE to 7.99% higher than the existing 6.89%. However, the commercialized phosphor have a particle size of 10 μm, and it is necessary to adopt nano-size phosphor in order to use DSSCs with 8 ~ 9 μm thick TiO_2 layer.

$YBO_3:Eu^{3+}$ phosphor is a type of red phosphor, which absorbs short wave of 245 nm and emits the visible light wave of 580 nm.[13] Since the size of particles may be varied depending on the thermal treatment temperature in the synthesis process, it is possible to produce nano-size phos-

†Corresponding author : Ohsung Song
E-mail : songos@uos.ac.kr
Tel : +82-2-6490-2410 Fax : +82-2-6490-2404

phor by optimizing the thermal treatment temperature.[14)]

In addition, it is reported that the transmittance of ultraviolet rays in a DSSC device is as much as 30 ~ 40% of the incident light. It is expected that the ECE can be improved by adopting the scattering layer with $YBO_3:Eu^{3+}$ phosphor that absorbs ultraviolet rays that would be lost in existing ways.[15)]

In this study, we adopted $YBO_3:Eu^{3+}$ phosphor having a nano particle size on scattering layers in DSSC to improving ECE.

2. Experimental Procedure

To examine the change of opto-electrical characteristics in a DSSC upon addition of $YBO_3:Eu^{3+}$ phosphor, 0 ~ 5 wt% of $YBO_3:Eu^{3+}$ whose particles were as small as 100 nm was added to the scattering layer and then distributed.

Nano-size phosphor particles were mixed for 5 h at 80°C after $Y(NO_3)_3 \cdot 6H_2O$ 3.8345 g(0.1 M), H_3BO_3 0.6493 g(0.105 M), $Eu(NO_3)_3 \cdot 5H_2O$ 0.2142 g(0.005 M) were dissolved in 100 ml of distilled water with 13 ml of ammonia solution (25%, NH_4OH) at pH 9. They were then cleansed by means of distilled water and ethanol and went through a thermal treatment at 800°C for 2 h to produce $YBO_3:Eu^{3+}$.

We analyzed the surface microstructure of nano-size phosphor by field emission scanning electron microscope (FE-SEM, S-4300, Hitachi) at an acceleration voltage of 15 kV.

To check the composition of producing phosphor, the high resolution X-ray diffraction analysis method (HRXRD, X' pert-pro, PANalytical) was used. The X-ray source was CuKα with a nickel filter. The tube current was 30 mA, and the acceleration voltage was 40 kV. The phosphor composition was examined in the 2θ range of 20° to 80°.

PL (Hitachi, F-4500) was utilized to check the fluorescence characteristics and emitted waves in the range of 200 to 800 nm. The excitation wavelength was set to 250 nm, the scan mode to emission, and the data mode to fluorescence respectively.

We produced 300 nm-thick blocking layers by mixing titanium(IV)bis(ethyl aceto acetato)-diisopropoxide and 1-butanol into a solution, followed by spin-coating for 500 rpm-10 sec. and 2000 rpm-40 sec., and then heat treating at 500°C for 15 min.

We fabricated the 10 μm-thick TiO_2 films by coating TiO_2 paste having particle size of 20 nm (DSL 18NR-T of 10, Dyesol) via doctor blade method, and by heat treatment at 500°C for 30 min. The scattering layer with 0 ~ 10 wt% of phosphor was coated by doctor blade method, and then it went through a thermal treatment at 500°C for 30 min to produce a 10 μm -thick scattering layer.

For a visual analysis, dark-field illumination on the sides and bottom of the sample was conducted in the range of 10 ~ 60 magnifications by means of a GIA optical microscope in addition to the overhead light and UV illumination at the top of the sample. The image was taken by means of a digital camera (Nikon, Coolpix4500).

The micro-Raman spectrometer (UniThink, UniRaman) was utilized to measure the major components: as the phosphor powder was put on a glass. At this time, characteristic peaks were checked for the range of 200 ~ 2000 cm^{-1} by conducting scans for 60 times/sec by using an accumulation mode at the center value of 1000 cm^{-1} for each sample.

We absorbed 0.5 mM cis-vis bis-ruthenium (II) bis-tetrabutylammonium (N719) to complete the working electrode of the glass/FTO/blocking layer/TiO_2/scattering layer + $YBO_3:Eu^{3+}$ / dye(N719).

The CE was prepared by RF sputter (MHS-1500, Moohan, 300 W, 13.56 MHz) to form a 100 nm-Pt film on a glass substrate using 99.99% Pt as a target. A flow of 40 sccm Ar at pressure of 5 mtorr at RT was set for the process.

With the produced working electrode and counter electrode fixed with clips, electrolytes were put in to complete the DSSC consist of glass / FTO / blocking layer / TiO_2 / scattering layer + $YBO_3:Eu^{3+}$ / dye(N719) / electrolyte / 100 nm Pt / glass with active area of 0.45 cm^2.

The impedance of DSSC was determined by solar simulator (PEC-L11, Peccell) and potentiostat (Iviumstat, Ivium) to verify interfacial resistance. The analysis was carried out in the frequency range of 10 mHz ~ 1 MHz applying AC voltage and collecting the current responses.

I-V (current-voltage) characteristic of DSSC was measured by the same instruments under a setup; a 100 W Xenon lamp was the illumination source at 1 sun (100 mW/cm^2) condition. From the I-V curves, short-circuit current density (J_{sc}), open-circuit voltage (V_{oc}), fill factor (FF), and ECE were evaluated. To keep the quantity of light constant, a 0.45 cm^2-large mask was made with black insulation tape and attached on the DSSC.

3. Results and Discussion

Figure 1 shows the XRD results of the $YBO_3:Eu^{3+}$ phosphor. The upper right inset is the FESEM image of the $YBO_3:Eu^{3+}$ phosphor at 80,000 magnifications. The result of XRD analysis shows that the plane directions of $YBO_3:Eu^{3+}$ are (100), (102), (004), (110), (112), (200), and (114) for 26.80, 33.70, 41.00, 47.70, 52.35, 55.80, and 64.60°, respectively. This result indicates that the $YBO_3:Eu^{3+}$ having nano-particle size successfully produced.[16)] In addition, the FESEM image in the upper right inset shows that the particles size of $YBO_3:Eu^{3+}$ phosphor are from 50 nm to 100 nm.

Figure 2 shows the PL analysis results in the wavelength of the produced $YBO_3:Eu^{3+}$ from 570 nm to 660 nm. The PL analysis shows that emission peak of $YBO_3:Eu^{3+}$ was shown in the wavelengths of 595, 610, 625, and 650 nm, which corresponds to the report of Dubey *et al.*[16)] We confirmed that $YBO_3:Eu^{3+}$ phosphor absorbs short wave of 245 nm and emits light to the area of red visible rays with range of 595 ~ 650 nm. Therefore, our results imply that $YBO_3:Eu^{3+}$ phosphor will improve the ECE of DSSC because of increasing light absorption in the area of red visible rays.

Figure 3 shows that the surface images of the scattering

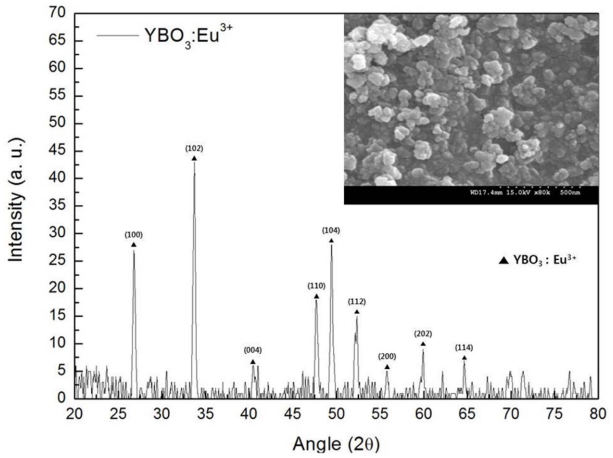

Fig. 1. XRD peak of fabricated $YBO_3:Eu^{3+}$. Inset is FESEM image.

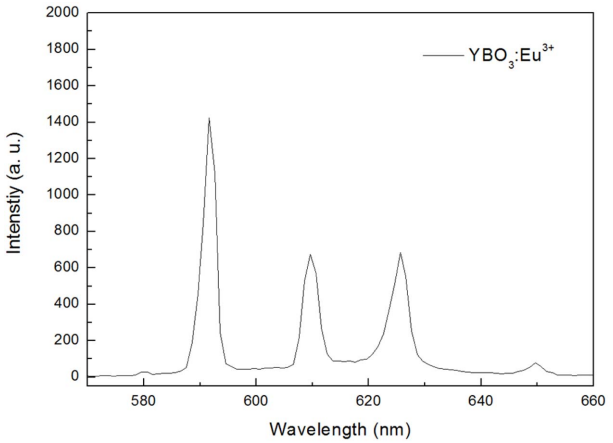

Fig. 2. Photoluminescence data of fabricated $YBO_3:Eu^{3+}$ in visible ray region.

layers with (a) 0 wt% and (b) 5 wt% of $YBO_3:Eu^{3+}$ phosphor under UV light. As for (a) 0 wt% phosphor employed to the scattering layer, the coating was uniform and no fluorescence was observed under UV irradiation. This result indicates that the only TiO_2 (scattering layer) does not have the fluorescence. As for (b) 5 wt% phosphor employed to the scattering layer, the spherical phosphor particles were uniformly dispersed compared to (a). In addition, the red light emission was observed from dispersed phosphor particles under UV irradiation. Thus, our results imply that $YBO_3:Eu^{3+}$ phosphor was successfully dispersed into the scattering layer.

Figure 4 shows that the FE-SEM images of WE with (a) 0 wt% and (b) 5 wt% of $YBO_3:Eu^{3+}$ phosphor at 500 magnifications. The upper right inset is a cross sectional FESEM image of the same WE at 4,000 magnifications. As for (a) 0 wt% of phosphor, the surface was uniformly coated without agglomeration, which corresponded to the result of previous Fig. 3. The cross sectional image in the upper right inset shows that both the scattering layer and TiO_2 layer were

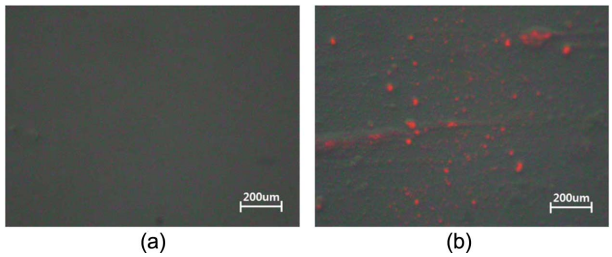

Fig. 3. Macro optical images of scattering layers with phosphor of (a) 0 wt%, and (b)5 wt% under UV irradiation.

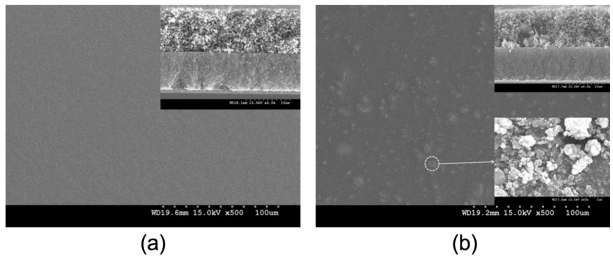

Fig. 4. FESEM images of scattering layers with phosphor of (a) 0 wt%, and (b) 5 wt%. Insets are cross sectional images.

coated properly as thick as 10 μm. As for (b) 5 wt% of phosphor, spherical particles were uniformly dispersed compared to (a). The $YBO_3:Eu^{3+}$ nano particles were condensed as small as 3 μm, as already shown in the Fig. 3. The cross sectional image in the upper right inset shows that both the scattering layer and TiO_2 layer were coated in the same thickness with (a). As indicated by the dotted circle, we confirmed the size of agglomeration was 3 μm. Thus, the FESEM analysis result demonstrates that $YBO_3:Eu^{3+}$ phosphor was successfully dispersed into the scattering layer as intended.

Figure 5 shows micro-Raman data of the WE samples with 0 ~ 5 wt% of $YBO_3:Eu^{3+}$ phosphor. The $YBO_3:Eu^{3+}$ phosphor showed Raman characteristic peaks at 1569, 1865, 1914, and 1948 cm^{-1}. In contrast, the Raman characteristic peak of $YBO_3:Eu^{3+}$ was not observed in the WE with 0 wt% of $YBO_3:Eu^{3+}$. In case of WEs with 1 ~ 5 wt% of $YBO_3:Eu^{3+}$ phosphor, the Raman characteristic peak of $YBO_3:Eu^{3+}$ was observed. As the amount of $YBO_3:Eu^{3+}$ increased, the intensity increased linearly. Thus, the Raman analysis result indirectly implied that the addition of $YBO_3:Eu^{3+}$ on the scattering layer was successfully dispersed as intended.

Figure 6 shows the Nyquist plot consisting of real part (Z') and imaginary part (Z'') obtained at an applied frequency for DSSC devices employing 0~10 wt% $YBO_3:Eu^{3+}$. As internal resistances of the common DSSC, three semicircles (R_1, R_2, R_3) were observed. R_1 values are the interface resistance that is related to the CE at 10^3-10^5 Hz, which is about 1.6 Ω within the error range. This is because the same CE was used in this study. R_2 values are related to the electron-transfer resistance in TiO_2 at 1-10^3 Hz, and it is shown to linearly

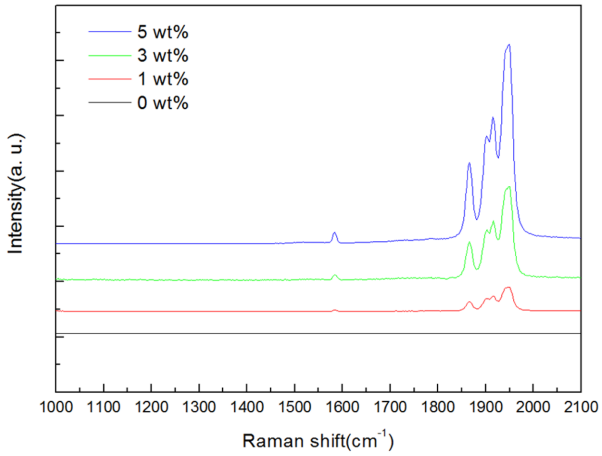

Fig. 5. Raman spectrums of working electrodes with scattering layers with phosphor of 0 wt% ~ 5 wt%.

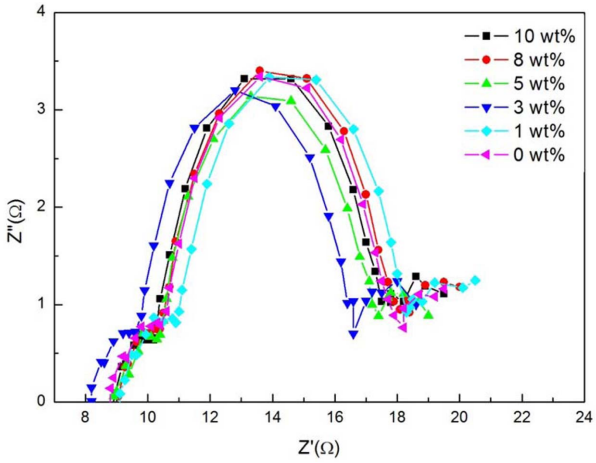

Fig. 6. Nyquist plot of DSSCs employing scattering layers with phosphor of 0 wt% ~ 10 wt%.

decrease upon increasing the amounts of 0, 1, 3, 5 wt% $YBO_3:Eu^{3+}$, respectively. As phosphor was dispersed on the scattering layer, ultraviolet rays were converted into visible rays, and as a result, light absorbance increased. However, R_2 values increased when the amounts of phosphor were more than 5 wt%, and this is attributed to a relative decrease in the fraction of TiO_2 (scattering layer). R_3 value represents the Warburg impedance, which is related to the diffusion of oxidation-reduction species in the electrolyte at above 10^6 Hz. R_3 value was approximately 1.6 Ω and was within the error range. The same electrolyte used for measurements should be responsible for this result. Thus, we confirmed that a proper amount of phosphor into scattering layer increased in additional light absorption and excited electrons, reducing the electron transport resistance.

Figure 7 shows the I-V data for the DSSC device with the structure of glass/FTO/blocking layer/TiO_2/scattering layer with 0 ~ 5 wt% $YBO_3:Eu^{3+}$/dye(N719)/electrolyte/100 nm Pt/glass. The J_{sc} of DSSC without phosphor was smaller than that of DSSC with phosphor. Especially as for 5 wt% phosphor, the value of J_{sc} was the largest.

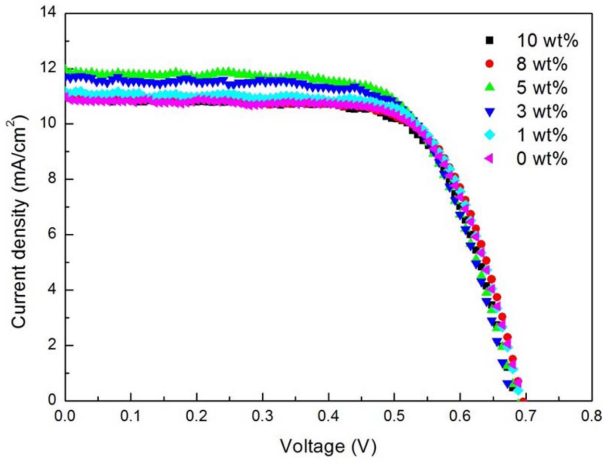

Fig. 7. Current-voltage (I-V) characteristic of DSSCs employing scattering layers with phosphor of 0 wt% ~ 10 wt%.

Table 1. Photovoltaic Properties and ECE of DSSC with Phosphor Addition

Sample	Voc (V)	FF	Jsc (mA/cm^2)	η (%)
0 wt%	0.69	0.69	10.96	5.00
1 wt%	0.69	0.66	11.18	5.12
3 wt%	0.68	0.65	11.71	5.17
5 wt%	0.68	0.64	11.96	5.20
8 wt%	0.69	0.66	11.02	5.07
10 wt%	0.68	0.66	10.97	4.98

Table 1 shows the I-V result of Fig. 7 in detail. V_{oc} showed similar values within the error range, and the similar values of V_{oc} considered to be attributable to the use of the same electrolyte in all Fermi levels as an element related to the oxidation-reduction reaction of the electrolyte. FF was affected by the interface resistance of elements, and was measured within the error range since the same TiO_2 paste, electrolyte, and CE were used in this study. J_{sc} of DSSC device employing 0 wt% phosphor was 10.96 mA/cm^2, and those of 1, 3, and 5 wt% phosphor were 11.18, 11.71, and 11.96 mA/cm^2, respectively. This indicates that as the amount of addition increased, the value of J_{sc} increased accordingly. As the result of the previous impedance analysis, employing 1 ~ 5 wt% phosphor makes possible additional light absorption in the ultraviolet range. As a result, the number of generated electrons increases. When a large amount of 8, 10 wt% phosphor was added, the values of J_{sc} decreased down to 11.02 and 10.97 mA/cm^2 due to a relative decrease in the fraction of TiO_2(scattering layer). Thus, the final ECEs obtained by employing 5 wt% phosphor were 5.20% depending on the increase in J_{sc}. Therefore, we successfully proposed DSSC devices with an improvement in ECE by employing phosphor of a proper quantity into scattering layer.

4. Conclusions

We employed $YBO_3:Eu^{3+}$ with particle size having 100 nm or smaller into the scattering layer of DSSC. $YBO_3:Eu^{3+}$ with particle size having 100 nm or smaller were produced and were uniformly dispersed into the scattering layer. As a result of analyzing the composition and fluorescence, it was demonstrated that $YBO_3:Eu^{3+}$ absorbed waves of 245 nm and emitted light in the range of visible rays. As for the ECE of DSSCs, DSSC device of employing 5 wt% phosphor was increased resulting from an increase in J_{sc}. In contrast, when a large amount of 8, 10 wt% phosphor was added, the values of ECE decreased due to a relative decrease in the fraction of TiO_2(scattering layer). Thus, by employing the appropriate amount of $YBO_3:Eu^{3+}$ phosphor, we have demonstrated an improvement in the ECE of DSSC.

REFERENCES

1. B. O'Regan and M. Grätzel, "A Low-Cost, High-Efficiency Solar Cell Based on Dye-Sensitized Colloidal TiO_2 Films," *Nature*, **353** [6346] 737-40 (1991).
2. Y.-W. Ok, A. D. Upadhyaya, Y. Tao, F. Zimbardi, K. Ryu, M. -H. Kang, and A. Rohatgi, "Ion-Implanted and Screen-Printed Large Area 20% Efficient N-type Front Junction Si Solar Cells," *Sol. Energy Mater. Sol. Cells,* **123** 92-6 (2014).
3. F. Gao, Y. Wang, D. Shi, J. Zhang, M. Wang, X. Jing, R. Humphry-Baker, P. Wang, S. M. Zakeeruddin, and M. Grätzel, "Enhance the Optical Absorptivity of Nanocrystalline TiO_2 Film with High Molar Extinction Coefficient Ruthenium Sensitizers for High Performance Dye-Sensitized Solar Cells," *J. Am. Chem. Soc.,* **130** [32] 10720-28 (2008).
4. K. Wongcharee, V. Meeyoo, and S. Chavadej, "Dye-Sensitized Solar Cell Using Natural Dyes Extracted from Rosella and Blue Pea Flowers," *Sol. Energy Mater. Sol. Cells*, **91** [7] 566-71 (2007).
5. M. A. Green, K. Emery, Y. Hishikawa, W. Warta, and E. D. Dunlop, "Solar Cell Efficiency Table," *Prog. Photovolt: Res. Appl.*, **22** [1] 701-10 (2014).
6. S. Zhang, H. Niu, Y. Lan, C. Cheng, J. Xu, and X. Wang, "Synthesis of TiO_2 Nanoparticles on Plasma-Treated Carbon Nanotubes and its Application in Photoanodes of Dye-Sensitized Solar Cells," *J. Phys. Chem.,* **115** [44] 22025-34 (2011).
7. M. K. Nazeeruddin, A. Kay, R. Humpbry-Baker, E. Miiller, P. Liska, N. Vlachopoulos, and M. Gratzel, "Conversion of Light to Electricity by cis-X2bis(2,2'-bipyridyl-4,4'-dicarboxylate)ruthenium(II) Charge-Transfer Sensitizers (X = Cl-, Br-, I-, CN-, and SCN-) on Nanocrystalline Titanium Dioxide Electrodes," *J. Am. Chem. Soc.,* **115** [14] 6382-90 (1993).
8. D. R. Huang, Y. J. Jiang, R. L, Liou, C. H. Chen, Y. A. Chen, and C. H. Tsai, "Enhancing the Efficiency of Dye-Sensitized Solar Cells by Adding Diatom Frustules into TiO_2 Working Electrodes," *Appl. Surf. Sci.,* **347** 64-72 (2015).
9. Y. Noh and O. Song, "Properties of the Scattering Layer Inserted Dye Sensitized Solar Cells," *Korea J. Met. Mater.*, **51** [10] 767-71 (2013).
10. E. Klampaftis, D. Ross, K. R. Mclntosh, and R. S. Richards, "Enhancing the Performance of Solar Cells via Luminescent Down-Shifting of the Incident Spectrum: A Review," *Sol. Energy Mater. Sol. Cells,* **93** [8] 1182-94 (2009).
11. N. Yao, J. Huang, K. Fu, S. Liu, D. E, Y. Wang, X. Xu, M. Zhu, and B. Cao, "Efficiency Enhancement in Dye-Sensitized Solar Cells with Down Conversion Material ZnO : Eu^{3+}, Dy^{3+}," *J. Power Sources,* **267** 405-10 (2014).
12. S. Bai, L. Liang, C. Wang, H. F. Mehnane, C. Bu, S. You, Z. Yu, N. Cheng, H. Hu, W. Liu, S. Guo, and X. Zhao, "A Novel Glowing Electrolyte Based on Perylene Accompany with Spectrum Compensation Function for Efficient Dye Sensitized Solar Cells," *J. Power Sources,* **280** 430-34 (2015).
13. R. S. Yadav, S. K. Pandey, and A. C. Pandey, "Improve Color Purity in Nano-Size Eu^{3+}-Doped YBO_3 Red Phosphor," *J. Lumin.*, **129** [9] 1078-82 (2009).
14. P. K. Sharma, R. K. Dutta, and A. C. Pandey, "Size Dependence of Eu-O Charge Transfer Process on Luminescence Characteristices of $YBO_3:Eu^{3+}$ Nanocrystals," *Opt. Lett.*, **35** [14] 2331-33 (2010).
15. Ma. Carnie, T. Watson, and D. Worsley, "UV Filtering of Dye-Sensitized Solar Cells: The Effects of Varying the UV Cut-Off upon Cell Performance and Incident Photon-to-Electron Conversion Efficiency," *Int. J. Photoenergy*, **2012** 506132 (2012).
16. V. Dubey, J. Kaur, S. Agrawal, N. S. Suryanarayana, and K. V. R. Murthy, "Effect of Eu^{3+} Concentration on Photoluminescence and Thermoluminescence Behavior of $YBO_3:Eu^{3+}$ Phosphor," *Superlattices Microstruct.,* **67** 156-71 (2014).